Simple Indoor Path Loss Prediction Algorithm and Validation in Living Lab Setting

**David Plets · Wout Joseph ·
Kris Vanhecke · Emmeric Tanghe ·
Luc Martens**

Abstract A simple heuristic algorithm has been developed for an accurate prediction of indoor wireless coverage, aiming to improve existing models upon multiple aspects. Extensive measurements on several floors in four buildings are used as validation cases and show an excellent agreement with the predictions. As the prediction is based on the free-space loss model for every environment, it is generally applicable, while other propagation models are often too dependent on the environment upon which it is based. The applicability of the algorithm to a wireless testbed network in a living lab setting with WLAN 802.11b/g nodes is investigated by a site survey. The results can be extremely useful for the rollout of indoor wireless networks.

Keywords indoor propagation · WLAN · algorithm · prediction

1 Introduction

The increasing use of indoor wireless systems, such as WLAN (Wireless Local Area Network) (broadcast) systems in e.g., conference rooms, office buildings,. . . or sensor networks [1] for network management, monitoring, security,. . . gives rise to a need for propagation prediction algorithms that can be used for different building types (office buildings, exhibition halls, factories,. . .), with a sufficient accuracy. The characterization of indoor propagation and path loss in indoor environments has been the subject of extensive research and many models have been proposed to make accurate predictions [2–26]. Different prediction approaches have been followed.

David Plets, Wout Joseph, Kris Vanhecke, Emmeric Tanghe, Luc Martens
Ghent University / IBBT, Dept. of Information Technology
Gaston Crommenlaan 8 box 201, B-9050 Ghent, Belgium
Fax: +32 9 33 14899
E-mail: david.plets@intec.UGent.be

Statistical (site-specific) one-slope models [15–23] (e.g. multi-wall models) predict path loss based on measurements of a specific site or for a specific environment. They are easy to construct when a lot of measurement data is available and allow a fast prediction. However, the validity of the prediction is mostly limited to the propagation environment it represents. In order to obtain a reliable prediction model for a new building type (or a new transmitter location), an additional measurement campaign will most likely have to be executed.

In [15,27], indoor path losses have been statistically investigated for different room categories (adjacent to transmitter room, non-adjacent,...) in 14 houses. Path loss in five office environments has been determined and the importance of taking wall attenuations into account in the prediction model is indicated in [16]. In [18], low prediction errors are obtained, but the analysis was performed for a site-specific validation of the ITU Indoor Path Loss model (only indoor office environments), whereas our algorithm is generally applicable (office environment, exhibition hall, retirement centre,...). In [20], different propagation models were tuned to a measurement set, but unlike in this paper, no validation measurements were performed. *Tuning* a prediction model can be understood as adapting the model parameters to make the predictions correspond with the path loss measurements that were performed. Unlike in many other works, no parameter tuning will be executed in the validation phase of our prediction model.

One-slope models and different multi-wall based models were analyzed and results have been provided for a typical office environment in [28]. The standard deviation of the model error was around 6 dB for the best model. In [21], a simple one-slope model was constructed for a mostly-LoS environment. A value of 2 for the path loss exponent n was obtained. LoS and NLoS measurements have been fitted to a one-slope model in [23]. The path loss exponent here accounted also for the wall losses for the NLoS measurements. However, no model validations in other rooms or buildings were executed. In [22], a statistical path loss model is proposed for different propagation conditions. No validation measurements have been performed to test the model.

To avoid the limited prediction validity of statistical models, *ray-tracing and ray-launching* model techniques [2–6] take into account the geometry of the building and the used materials. They usually require a vector based description of the environment to identify the reflected and diffracted rays from surface and edges [29]. Although ray-tracing solvers claim to be accurate, the results appear to be very dependent on geometrical details of the ground plan, which force the user to work with very accurate plans [30]. Moreover, the prediction transmission settings (number of interactions (transmissions, reflections, and diffractions) of the rays with the environment) may have a relevant influence on the prediction results: differences up to 5 dB have been observed for the average path loss along a line-of-sight (LoS) path when the number of interactions is adapted [31]. Finally, for large buildings, prediction times can run into several hours.

In [2], ray-tracing is used for indoor path loss prediction, with a distinction

between LoS and NLoS. Procentual prediction errors range from 5% to 10%, which is higher than for our prediction. Different ray-tracing approaches (field-sum and power-sum) have been investigated in [5]. Field-sum appeared to be most accurate. In [3,4], efficient two-dimensional ray-tracing algorithms for an indoor environment have been presented, resulting in a significant reduction in the computational time, without losing prediction accuracy.

*Numerical solver model*s [7–10] consist of screen or integral methods, Finite-difference time-domain (FDTD),...[29]. Numerical solvers also have the disadvantage of a long calculation time, and the large dependence of the results on the precision of the ground plan. Also, the dielectric material properties of the environment have to be accurately known to obtain a good prediction.
A theoretical waveguide model permitting a rigorous modal solution is proposed for predicting path loss inside buildings in [7].

Our prediction algorithm can be classified as a heuristic algorithm. *Heuristic predictions* [11–14] are based on one or more rules of thumb in order to make a path loss prediction.
Heuristic approaches have been proposed in [12–14]. An indoor propagation model making use of the estimation of the transmitted field at the corners of each room is presented in [12]. Good results (mean absolute prediction error of 2.2 dB) are obtained, but the model is less suitable for environments where diffraction is the dominant mechanism. A more complex version of the dominant path loss model (using more model parameters) is studied and calibrated in order to minimise the prediction errors for a certain building in [13]. In [14], a WLAN planning tool was developed to optimize the position and number of access points, as well as the total cost of the required equipment, according to different WLAN suppliers, in indoor and outdoor environments.
The heuristic indoor path loss prediction model we are presenting is both simple and quick (as the statistical models), but will also prove to be very accurate (as numerical and ray-tracing solvers claim to be), although no tuning of the model will be performed in the model validation phase. Furthermore, our model is also valid for different building types. The proposed algorithm avoids the quoted problems of the statistical and ray-tracing methods by determining the dominant path between transmitter and receiver [11,32]. Compared to [11, 32], adaptations such as path loss model simplification, the avoidance of neural networks, and a physically intuitive approach are carried out. The simplified approach is proposed without losing prediction accuracy: the obtained deviations are lower than only 3 dB. A measurement campaign has been executed on several floors in four buildings in Belgium for construction and extensive validation of the propagation model. As our algorithm is based on free-space loss for every environment, the algorithm is generally applicable, while other predictions are often too dependent on the environment upon which the used propagation model is based. The applicability of the algorithm to a wireless living lab with WLAN 802.11b/g nodes is investigated by a site survey. We aim to provide an physically intuitive, yet accurate prediction of the path loss

for different types of public and office buildings. The prediction algorithm can be of great interest to anyone who wants to set up a WLAN, sensor, or broadcast network in either home or professional environments [33].

Section 2 describes the investigated buildings and their use in the propagation modeling procedure. In Section 3, the measurement setup is described, and in Section 4, the prediction algorithm is presented. The modeling of the path loss parameters is discussed in Section 5 and Section 6 investigates different validation cases. In Section 7, the applicability of the model to a wireless living lab is discussed. Finally, conclusions are presented in Section 8.

2 Investigated buildings

In this paper, an indoor path loss model for the 2.4 GHz-band will be formulated. To determine the model parameters, PL measurements and simulations have been performed in four very different buildings, named Zuiderpoort (I), De Vijvers (II), Lamot (III), and Vooruit (IV). The characteristics of the investigated buildings are described hereafter and are summarized in Table 1 at the end of this section.

Zuiderpoort is a modern three-storey office building, with movable walls (layered drywalls) around a core consisting of concrete walls (Table 1). Fig. 1 shows the third floor of this building. Path loss measurements have been performed on both floors (1,581 path loss samples on the second floor and 5,078 samples on the third floor). The orange walls are layered drywalls, the grey ones are made of concrete. In order to assure the validity of the predictions for the entire building floor, trajectories T1-T5 are chosen to represent LoS, obstructed line-of-sight (OLoS), as well as NLoS propagation cases, while rooms A-H are chosen to investigate propagation through subsequently adjacent rooms. In rooms A-H, an average path loss in the room is calculated by moving the receiver antenna randomly through the room during 2 minutes. For the measurements on the third floor (Fig. 1), T_A is the access point for measurement trajectories T1-T5 and T_B for measurements in rooms A-H and for measurement trajectory 'corr' (corridor).
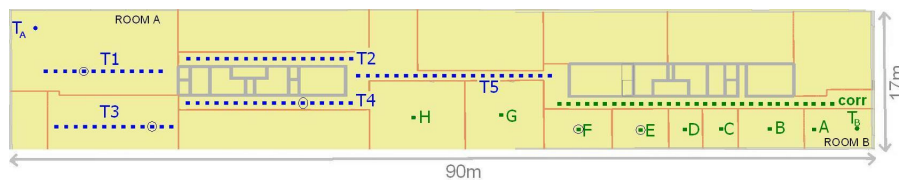

Fig. 1 Measurement trajectories on the third floor of the Zuiderpoort office building. The points for which the different path loss contributions are investigated in Table 3 are circled on T1, T3, T4, and in rooms E and F.

De Vijvers is a retirement home (Table 1), where 7,095 measurement samples were collected along twelve trajectories (T1 - T12) on the ground floor (see Fig. 2). The building mainly consists of concrete walls. Both LoS and NLoS trajectories are chosen to investigate the path loss prediction. Trajectory T12 is a part of trajectory T1, but for T1, T_A was the active transmitter, whereas for all other trajectories (T2-T12), T_B was active.
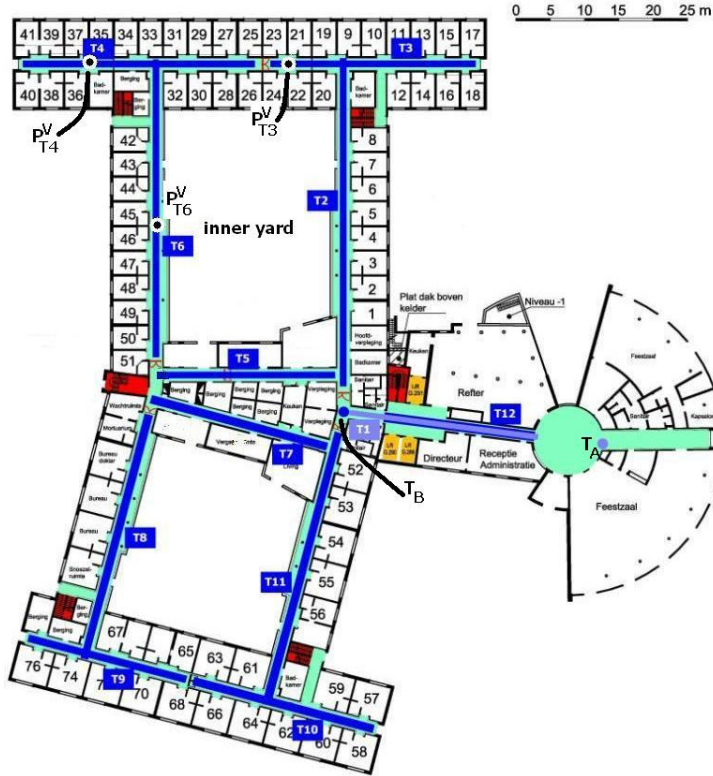

Fig. 2 Ground plan of 'De Vijvers' with indication of transmitters T_A and T_B and the measurement trajectories T1-T12. The points for which the different path loss contributions are investigated in Table 3 are indicated on T3, T4, and T6 with a black dot within a white dot.

Lamot is a multi-storey congress and heritage centre with multipurpose rooms for conferences, seminars, workshops, fashion shows, product presentations,... Thirteen path loss measurement trajectories (4,070 samples) have been executed on the third floor and the fifth floor, both having a similar geometry. The building is mainly constructed with concrete walls. Both LoS and NLoS trajectories are chosen to investigate the path loss prediction.

Vooruit is a polyvalent arts centre for all kinds of events (concerts, par-

ties, debates, ...), built between 1911 and 1914. Measurements are performed on three floors (ground floor, first floor, and second floor). This building also mainly consists of concrete walls, some of them even with a thickness of 50 cm. Seventeen trajectories (4,390 samples) have been traversed for the path loss measurements in this building. Mostly NLoS predictions are chosen to investigate the path loss prediction.

It is clear that these buildings have very different characteristics. It will be shown that our approach is capable to predict path loss for these different indoor environments.

ID	name and description	dominant materials	measured floors	goal
I	**Zuiderpoort** (office building)	layered drywall, concrete	2nd	PL measurement (tuning)
			3rd	PL measurement (validation)
II	**De Vijvers** (retirement home)	concrete	ground floor	PL measurement (validation+interaction loss tuning)
III	**Lamot** (congress centre)	concrete	3rd	PL measurement (validation)
			5th	PL measurement (validation)
IV	**Vooruit** (arts centre)	concrete, glass	ground floor	PL measurement (validation)
			1st	PL measurement (validation)
			2nd	PL measurement (validation)

Table 1 Overview of the characteristics of the investigated buildings.

3 Path loss measurements

The path loss prediction models incorporated in the prediction algorithm are based upon, and validated with path loss measurements in different buildings. This section discusses the setup for these path loss measurements and their reproducibility.

As Tx an omnidirectional Jaybeam antenna type MA431Z00 with a gain of 4.2 dBi is used [34]. The Tx is placed at a height of 2.5 m above ground level (typical access point height in public environments). It is fed with a continuous sine wave at 2.4 GHz (ISM-band, typical for WLAN communication) with an EIRP of 20 dBm. Possible interfering sources (e.g., WiFi networks) are desactivated in order not to influence the measurements. The receiver antenna (identical to Tx) is attached to a cart at a height of 1 m (typical user device height) and is connected to a Rohde & Schwarz FSEM30 spectrum analyzer with a frequency range from 20 Hz up to 26.5 GHz. The output of the SA is sampled and stored on a laptop used to record and process the measurement data. Fig. 3 shows the measurement setup.
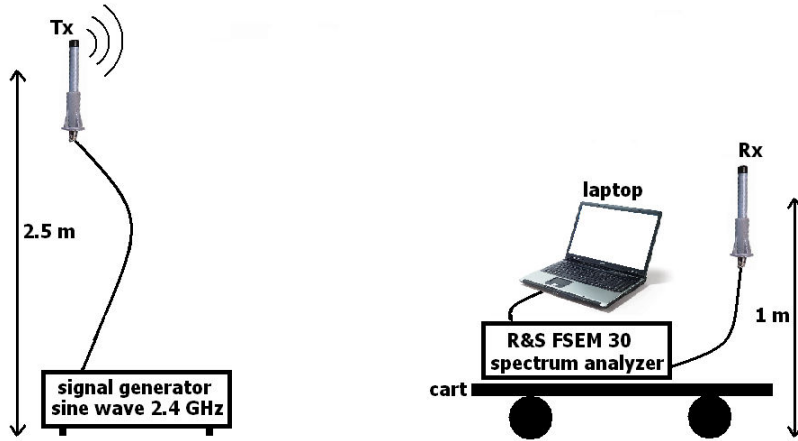
Fig. 3 Measurement setup.

Since the model parameters are based almost solely on the path loss measurements performed on the second floor of the Zuiderpoort building, it is important that the measured path loss values are reliable. Therefore, we investigate the reproducibility of the measurements by executing them four times (Meas1 to Meas4 in Table 2) for each of the five trajectories (three times for T2 due to practical reasons).

Table 2 shows the average path loss recorded along T1-T5 for the four measurements. The five averages of these four measurements are used to determine the model parameter for the interaction loss (A in eq. (2)). Table 2 shows that the maximum deviation from the average path loss $\triangle_{\mathrm{max}}$ varies only from 0.53 dB to 1.49 dB, indicating that one measurement suffices to give a correct estimate of the path loss along a trajectory. These average values will be used to determine the model parameters in Section 5.

	T1	T2	T3	T4	T5
Meas1	56.56	56.64	62.53	69.38	79.11
Meas2	55.95	59.04	63.17	69.04	78.26
Meas3	55.67	58.71	63.08	68.11	78.48
Meas4	57.00	-	63.44	69.36	78.45
mean	56.30	58.13	63.06	68.97	78.57
$\triangle_{\mathbf{max}}$	0.70	1.49	0.53	0.86	0.54

Table 2 Reproducibility of the measured path loss along T1-T5.

4 Algorithm concept and implementation

In this section, the concept and the implementation of the prediction algorithm is discussed. Our goal is to develop an accurate and fast algorithm that does not make use of extensive fitting to obtain good predictions, as this often leads to results which are only usable for the investigated building.

The planning algorithm predicts the indoor coverage by means of a path loss (PL) prediction based on the Indoor Dominant Path Model (IDP) [11, 32]. This model is a compromise between semi-empirical models only considering the "direct" ray between transmitter Tx and receiver Rx (e.g., multi-wall model) and ray-tracing models where hundreds of rays and their interactions with the environment are investigated. In the IDP model, propagation focuses on the dominant path between transmitter and receiver, i.e., the path along which the signal encounters the smallest obstruction in terms of path loss. It takes into account the length along the path, the number and type of interactions (e.g., reflection, transmission, etc.), the material properties of the objects encountered along the path, etc. The approach of using the IDP model is justified by the fact that more than 95% of the energy received is contained in only 2 or 3 rays [11]. According to [11], predictions made by IDP models reach the accuracy of ray-tracing models or even exceed it.

4.1 Comparison with the IDP model

Different propagation properties can be chosen to be included into the IDP model. We have chosen to take into account the distance along the dominant path (distance loss), the corresponding wall losses, and the propagation direction changes along the dominant path (interaction loss). The IDP model as presented in [32] also adds other factors, such as waveguiding, transmitter room size,... The more factors used though, the more tuning is needed (limited general use) and the more difficult it is to determine the influence of each single factor on the path loss. As a result, neural networks are mostly needed to construct a path loss model. Also, the more influencing factors included, the higher the dimensions of the problem, and the more training patterns needed to construct reliable models. Moreover, unlike with neural networks, these contributions are physically in line with the actual path loss caused by the three factors, which makes it easier to a posteriori adapt e.g., penetration losses based on new measurements or add new wall types to the path loss model. Therefore, we aimed to construct a model as simple as possible, but as complex as necessary for accurate predictions, this way improving the IDP model from [11, 32]. In Sections 5 and 6, it will be demonstrated that the proposed three contributing factors suffice to perform solid predictions.

4.2 General path loss model

The path loss model, based on the three discussed contributions (distance loss, cumulated wall loss, interaction loss), will now be discussed. Path losses are determined between the transmit antenna of an access point and a receiving antenna at a certain location. The total path loss for a path between an access point in one room and a receiver location in another room, is the sum of the the distance loss along the path, the total wall loss along the path, and the interaction loss along the path. The total path loss of a certain path can thus be calculated as follows:

$$
\mathrm{PL} \;=\; \underbrace{\mathrm{PL}_0 + 10\,\mathrm{n}\,\log(\frac{\mathrm{d}}{\mathrm{d}_0})+}_{\text{distance loss}} \quad \underbrace{\sum_{\mathrm{i}} \mathrm{L}_{\mathrm{W_i}}}_{\text{cumulated wall loss}} \quad + \quad \underbrace{\sum_{\mathrm{j}} \mathrm{L}_{\mathrm{B_j}}}_{\text{interaction loss}} \quad , \qquad (1)
$$

where PL [dB] is the total path loss along the path, PL_0 [dB] is the path loss at a distance of d_0 according to the distance loss model, d [m] is the distance along the path between access point and receiver, d_0 [m] is a reference distance, and n [-] is the path loss exponent. d_0 was chosen 1 m here. The first two terms of the sum represent the path loss due to the distance along the considered path, noted here as the "distance loss". It is calculated for a certain path as the path loss at a distance equal to the length of the path that traverses all the walls of the considered path. $\sum_{\mathrm{i}} \mathrm{L}_{\mathrm{W_i}}$ is the "cumulated wall loss" along the path (i.e., the sum of the wall losses $\mathrm{L}_{\mathrm{W_i}}$ of all walls $\mathrm{W_i}$ traversed along the path, i = 1,..., W, where W is the total number of walls along the path). $\sum_{\mathrm{j}} \mathrm{L}_{\mathrm{B_j}}$ is the "interaction loss", i.e. the cumulated loss $\mathrm{L}_{\mathrm{B_j}}$ caused by all propagation direction changes $\mathrm{B_j}$ of the propagation path from access point to receiver, with j = 1,..., B, where B is the number of times the propagation path changes its direction. The **dominant path** is defined as the path for which the sum of the cumulated wall loss, the distance loss, and the interaction loss is the lowest. Values for the model parameters will be determined in Section 5. Typical contributions of the distance loss, cumulated wall loss, and interactions loss for different transmitter-receiver configuratons will be presented in Section 4.3.

4.3 Judiciously chosen and physically intuitive path

Our model was aimed at an intuitive understanding of how path loss is affected, without losing accuracy. The three contributions taken into account in the model of equation (1) (distance loss, cumulated wall loss, and interaction loss) are selected based on the real physical propagation of a wave between transmitter and receiver.

To gain more insight into the model, we will now investigate the contributions to the total path loss of the three factors, for eight different transmitter-receiver configurations: five points circled in Fig. 1, and three points indicated with a black dot within a white dot in Fig. 2 in the building of De Vijvers (retirement home in Ghent, Belgium, see Section 2). Table 3 shows the three different contributions to the total path loss for each of these points P_T^B, where B indicates the building where the point is located (Z = Zuiderpoort or V = De Vijvers) and T indicates the trajectory on which or the room in which the point is located. This table also shows the dominant path from transmitter to receiver. Different propagation situations are illustrated: LoS (P_{T1}^Z), OLoS (obstructed line-of-sight) with one (P_{T3}^Z) or more (P_E^Z) walls between Tx and Rx, and propagation through corridors and/or rooms (all other points). In all cases, the distance loss is by far the most dominant factor. As the cumulated wall loss increases, it becomes more likely that another path (through corridors) will be dominant. In the De Vijvers building (containing a lot of concrete walls), the interaction losses can be quite high (up to 17.2 dB for P_{T4}^V).
Our model was aimed at an intuitive understanding of how path loss is affected, without losing accuracy.

Rx point	Tx	DL [dB]	CWL [dB]	IL [dB]	PL [dB]	Dominant path
P_{T1}^Z	T_A	57.0	0	0	57.0	direct ray
P_{T3}^Z	T_A	64.1	2.0	0	66.1	direct ray
P_{T4}^Z	T_A	69.5	4.0	1.9	75.4	through room of P_{T3}^Z
P_E^Z	T_B	67.4	8.0	0	75.4	direct ray
P_F^Z	T_B	70.0	6.0	3.0	79.0	through corridor and room of P_E^Z
P_{T3}^V	T_B	75.2	2.0	17.0	94.2	through corridors along T2 and T3
P_{T4}^V	T_B	78.7	2.0	17.2	97.9	through corridors along T2, T3, and T4
P_{T6}^V	T_B	73.8	6.0	15.0	94.8	through corridor along T2, then crossing the inner yard

Table 3 Overview of the three different contributions (DL = Distance Loss, CWL = Cumulated Wall Loss, IL = Interaction Loss) to the total path loss PL between eight receiver points and the transmitter in two buildings.

5 Modeling the parameters of the dominant path model

In this section, the model parameters will be determined. The four buildings described in Section 2 are used for the construction and the validation of the path loss model. We have deliberately chosen different types of buildings (modern office building, retirement home, modern congress centre with large exhibition halls, and old arts centre), in order to investigate the general applicability of the model. Path loss measurements on the different investi-

gated building floors are used either for tuning the model parameters or for validation purposes (see Table 1, column 'goal').

5.1 Distance loss

A first limitation we impose ourselves is the use of the free-space loss model for the **distance loss** (see equation (1): n = 2, PL_0 = 40 dB, d_0 = 1 m), because we aim to use a general model, avoiding fitting and tuning of the model to agree with existing measurement data of a certain environment. This way, we intend to increase the general applicability of equation (1). Changing these parameters might probably improve the prediction accuracy in the model tuning phase, but it is more likely that the resulting model would be too specific for a specific building (type), something we try to avoid in this research. The free-space loss model seemed like a good starting point for a general prediction model. Results will indicate that this was a feasible choice.

5.2 Cumulated wall loss

For the determination of the term representing the **cumulated wall loss** (see equation (1), we have first measured the penetration loss of the two wall types present in the Zuiderpoort building, layered drywalls (orange walls in Fig. 1) and concrete walls (grey walls in Fig. 1), and we have used the (rounded) values in the model, 2 dB and 10 dB respectively. For other wall types, we have based the loss values on available literature. For glass (windows or glass doors), 2 dB was used [35]. The importance of correct wall penetration loss values is demonstrated in [29]. A distinction was made between thin (< 15 cm) and thick (> 15 cm) walls. For thick concrete walls a loss of 15 dB [36] was used. The model's penetration loss database can easily be extended with penetration losses for various other materials using numbers and tables of [35–37].

5.3 Interaction loss

Based on the contribution of the distance loss and wall loss factor obtained as explained above, the value of the third factor, the **interaction loss** factor (see equation (1)), was adjusted in order to match the predictions to measurements performed on the second floor of the Zuiderpoort building. The measurements on this building floor were thus used to tune the model (see Table 1, column 'goal') and allowed us to determine the relation between the angle made by a propagation path and the additional loss associated with the propagation direction change. Because the interaction loss should be the same for e.g., three changes of 30° and one change of 90°, a linear relationship is proposed.

$$L_{B_j} = A \cdot \hat{B}_j \tag{2}$$

where L_{B_j} [dB] is the loss caused by bend B_j, A [dB/°] is a parameter depending on the dominant material in the building and $\hat{B}_j$ [°] is the angle corresponding with bend B_j. Based on measurements in two perpendicular corridors, A was determined at 0.0556 dB/° or 5 dB/90° for the Zuiderpoort (see Fig. 1) building, consisting mainly of layered drywalls.

5.4 Parameter values for the buildings used for validation

With the model parameters for distance loss, cumulated wall loss, and interaction loss now fixed, measurements on the third floor of the Zuiderpoort building were performed as a first validation without any further tuning (see Table 1), albeit in a very similar environment.
However, for the De Vijvers building, an environment mainly consisting of concrete walls (vs. the lighter layered drywalls in the Zuiderpoort building), the loss when propagating around corners appeared to be higher than for the Zuiderpoort building. The interaction loss for this environment was tuned to a value of 0.1946 dB/° or 17.5 dB/90° for concrete walls. In fact, it was only tuned for one of the twelve trajectories (T5, a trajectory where the dominant path made a propagation direction change), so all other measured trajectories in this building can be considered as validation trajectories as well (see Table 1, column 'goal').
For the remaining two buildings (Lamot and Vooruit), all model parameters from the analysis of the Zuiderpoort and De Vijvers buildings were used unchanged. Both buildings mainly consist of concrete, so we could immediately use the interaction loss function from the De Vijvers building, and validate the model with new measurements, without any additional tuning. Sections 5.5 and 6 will demonstrate that these validation results are more than satisfactory. Table 1 summarizes the goal (model tuning and/or validation) of the measurements in the different buildings.

5.5 Model performance for second floor of Zuiderpoort building

The model of eq. (1) with its parameters chosen as explained above is now used to calculate the deviations between the algorithm predictions and the measurements for the second floor of the Zuiderpoort building.
Table 4 shows for all trajectories on the second floor (used for modeling) and third floor (used for validation) the measured average path loss PL_{ms} [dB], the predicted path loss PL_{pr}, and the deviation δ [dB] for the considered model for Tx and Rx at heights of 2.5 m and 1 m respectively. δ [dB] is defined as follows.

$$\delta[dB] = PL_{pr}[dB] - PL_{ms}[dB] \tag{3}$$

Small deviations are obtained in Table 4 for the Zuiderpoort building. An average for the absolute value of the deviation $|\delta|$ is 1.77 dB for the second

floor. The deviation δ has an average of -1.15 dB with a standard deviation of 2.33 dB. Values for the standard deviation of 3 dB to 6 dB are considered to be excellent according to [29]. Our prediction model performs much better than this requirement.

Table 4 Measured average path loss PL$_{ms}$ [dB] along different trajectories, predicted average path loss PL$_{pr}$ [dB] and their deviations δ [dB] from PL$_{ms}$ in four buildings (building floor is indicated between brackets for trajectories with the same name). Average absolute deviations $|\delta|_{avg}$, average deviations δ_{avg}, and standard deviation σ of the deviations δ (see eq. (3)) indicated in bold (number between brackets indicates building floor, ZP = Zuiderpoort).

Zuiderpoort

	PL$_{ms}$ [dB]	PL$_{pr}$ [dB]	δ [dB]
T1(2)	56.3	61.1	-4.8
T2(2)	58.1	59.9	-1.8
T3(2)	63.1	62.8	0.3
T4(2)	69.0	67.7	1.3
T5(2)	78.6	79.3	-0.7
A	50.3	53.3	-3.0
B	61.7	61.4	0.3
C	64.1	67.4	-3.3
D	65.9	71.3	-5.4
E	68.6	75.4	-6.8
F	79.6	79.0	0.6
G	82.3	78.6	3.7
H	84.9	81.8	3.1
corr	66.9	66.9	0.0
T1(3)	58.1	59.1	-1.0
T2(3)	70.1	70.2	-0.1
T3(3)	65.5	65.2	0.3
T4(3)	78.9	73.5	5.4
T5(3)	79.7	76.9	2.8

	$|\delta|_{avg}$	δ_{avg}	σ
ZP(2)	1.77	-1.15	2.33
ZP(3)	2.56	-0.24	3.47

Vijvers

	PL$_{ms}$ [dB]	PL$_{pr}$ [dB]	δ [dB]
T1	66.6	66.7	-0.2
T2	68.8	68.8	0.0
T3	91.3	92.0	-0.7
T4	96.9	97.0	-0.1
T5	83.4	83.4	0.0
T6	99.3	96.7	2.6
T7	84.5	82.0	2.4
T8	97.6	99.7	-2.1
T9	100.6	95.5	5.1
T10	96.2	91.7	4.5
T11	70.4	67.8	2.5
T12	64.4	63.8	0.6

	$|\delta|_{avg}$	δ_{avg}	σ
Vijvers	1.73	1.22	2.19

Lamot

	PL$_{ms}$ [dB]	PL$_{pr}$ [dB]	δ [dB]
T1(3)	64.2	61.4	2.9
T2(3)	65.2	64.1	1.1
T3(3)	63.4	62.7	0.8
T4(3)	64.1	61.2	2.9
T5(3)	74.4	74.5	-0.1
T6(3)	87.1	85.7	1.4
T7(3)	83.1	80.2	2.8
T1(5)	60.4	60.4	0.0
T2(5)	63.1	63.9	-0.8
T3(5)	62.9	62.1	0.8
T4(5)	61.1	60.1	1.1
T6(5)	87.4	85.5	1.9
T7(5)	79.0	79.1	-0.2

	$|\delta|_{avg}$	δ_{avg}	σ
Lamot	1.29	1.12	1.23

Vooruit

	PL$_{ms}$ [dB]	PL$_{pr}$ [dB]	δ [dB]
T1(0)	61.3	59.6	1.8
T2(0)	73.4	67.0	6.4
T3(0)	77.5	78.0	-0.4
T4(0)	82.8	80.3	2.5
T5(0)	60.8	57.8	3.0
T6(0)	77.0	76.4	0.7
T7(0)	81.7	78.2	3.5
T1(1)	71.8	67.0	4.8
T2(1)	68.8	72.1	-3.3
T1(2)	74.4	74.1	0.4
T2(2)	71.1	66.1	5.0
T3(2)	67.9	63.5	4.4
T4(2)	83.1	78.7	4.4
T5(2)	86.2	83.0	3.3
T6(2)	69.9	65.4	4.4
T7(2)	66.1	62.4	3.7
T8(2)	71.3	71.7	-0.4

	$|\delta|_{avg}$	δ_{avg}	σ
Vooruit	3.08	2.60	2.49

6 Validation of path loss model with measurements in other buildings

The parameter values of our prediction model are based on measurements on one floor of one building (second floor, Zuiderpoort, see Section 5). In this section, we validate the general applicability of the path loss model constructed in Section 5, by comparing with measurements on another floor of the Zuiderpoort building, but also in the three other buildings presented in Section 2. Table 4 summarizes for trajectories in all buildings the measured average path loss PL_{ms} [dB], the predicted path loss PL_{pr} [dB], and the deviation δ [dB] = PL_{pr} - PL_{ms} for the considered model for Tx and Rx at heights of 2.5 m and 1 m respectively. It also gives a summary of the average absolute deviations $|\delta|_{avg}$, the average deviations δ_{avg}, and standard deviation σ of the deviations for each of the buildings.

The measurement trajectories on the **third floor of the Zuiderpoort building** (see Fig. 1) serve as a first validation for the model proposed in Section 5 (based on measurements on second floor of Zuiderpoort building). The low deviations ($|\delta|$ = 2.56 dB, δ = -0.24 dB, σ = 3.47 dB) show that the obtained prediction model is valid for a similar propagation environment (same building, but other floor, similar materials used) without tuning of the parameters in contrary to e.g., [38].

The measurement campaign of twelve trajectories on the ground floor in '**De Vijvers**' (see Fig. 2), a retirement home, has been considered as a second validation case. Table 4 shows that the predictions match the measurements excellently ($|\delta|$ = 1.73 dB, δ = 1.22 dB, σ = 2.19 dB). The deviations are small especially for the trajectories with the lowest path losses (T1, T2, T11, T12 are LoS or OLoS) which will be most relevant for actual networks (locations on trajectories with PL > 90 dB will probably have no WiFi reception).

The measurement campaign of thirteen trajectories on the third and fifth floor in congress centre '**Lamot**' has been considered as a third validation case, and the measurement campaign of seventeen trajectories on three floors of arts centre '**Vooruit**' as a fourth validation case. Just like for 'De Vijvers', predictions are very accurate (see Table 4), indicating that the proposed model is also valid for environments for which the model has not been tuned.

Table 4 shows the accuracy of our propagation prediction, even for buildings where no tuning at all has been performed (Lamot and Vooruit). In e.g.,[11], the obtained deviations are similar, but there, δ was considered, while we used $|\delta|$, which is more correct. Moreover, the values in [11] were obtained for a similar environment, whereas we have investigated different environments, indicating the improvement compared to [11].

7 Applicability to a wireless network in a living lab setting

In this section, it is investigated if the propagation model can be used to predict the path loss at the locations of the (fixed) nodes of a wireless (video)

living lab. The testbed network and the setup for the performed measurements will be presented, followed by an investigation of the prediction quality.

7.1 Living lab network

34 WLAN nodes have been put up at a height of 2.5 m in different rooms on the third floor of the Zuiderpoort office building in Ghent, Belgium (see Section 2). Fig. 4 shows the location of all WLAN nodes on this floor (90 m x 17 m). The nodes are Alix 3C3 devices running Linux. These are embedded PC's equipped with a Compex 802.11b/g WLM series MiniPCI network adapter. The wireless network interface is connected to a vertically polarized quarter-wavelength omnidirectional dipole antenna with a gain of 3 dBi. An 802.11b signal is transmitted by node 31 (indictated with circle in Figure 4) with a power of 0 dBm at a data rate of 1 Mbps. In total, 9000 packets are broadcast at a rate of 10 packets/s. In this validation procedure, all other nodes are receiving nodes measuring the Received Signal Strength Indication (RSSI). This RSSI value is then converted to a received power, based on a calibration performed in our lab. While space variability will inevitably be present due to the fixed character of the nodes (see also [39]), this procedure at least allows to average out the time variability present in the UHF band [40].
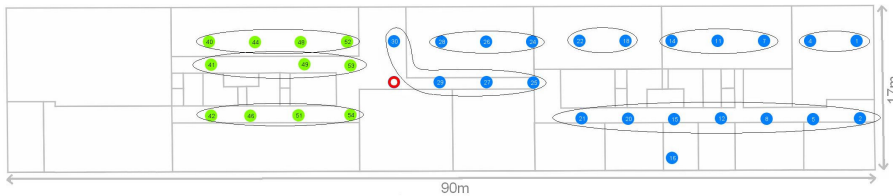

Fig. 4 Living lab node locations on third floor of Zuiderpoort building (transmitter located roughly in middle of building floor, indicated with circle).

7.2 Results

Path loss measurements with the spectrum analyser are executed close to these node locations (distance less than 30 cm). These obtained PL values are compared with the algorithm prediction and with the path loss values PL_{lab} measured by the nodes themselves (see Section 7.2). Nodes in the same room or nodes close to each other will also be investigated as a group as shown in Fig. 4 in order to obtain an averaged value, since the node locations are subject to small-scale fading mechanisms, which are not taken into account in the algorithm.

Fig. 5 shows the path loss $\text{PL}_{\text{pred}}^{2.5\,\text{m}}$ predicted by our algorithm and the path

loss PL_{SA} measured by the spectrum analyzer, as a function of the path loss PL_{lab} measured by the nodes for the different node groups. Perfect agreement is represented by the full line. Table 5 shows the mean deviations δ_{mean} and standard deviations σ between the SA measurement, prediction, and node measurements. Table 5 shows that the mean deviations vary between -0.27 and -2.14 dB when all nodes are considered separately, with standard deviations between 4.72 and 6.96 dB. When nodes are grouped, both the mean deviations (maximum of 1.56 dB) and the standard deviations (maximum of 4.65 dB) are lower (see Fig. 5 and Table 5).

In general, the predictions have a good correspondence with the node measurements. The mean deviation approaches 0 dB and the standard deviation corresponds with common shadowing margins. A first reason for the existing deviations is indeed the influence of fading mechanisms. Since in total, we only dispose of 33 measurements executed at one point location, it is impossible to average out the small-scale fading for each zone (most considered groups consist of only 2 to 4 locations, see Fig. 4). This is probably also why the predictions have lower deviations than the SA measurements, probably because the prediction is based on an average path loss in an area, while the SA measurements are more subject to fading mechanisms. Secondly, the path loss close to the transmitter (low path losses) is somewhat overestimated by the propagation model (see also T1(2) in Table 4, column 'Zuiderpoort'). The phenomenon of received powers being higher than expected close to the transmitter is also reported in [41].

We can thus conclude that it is possible to predict path losses for WLAN nodes in a living lab network.
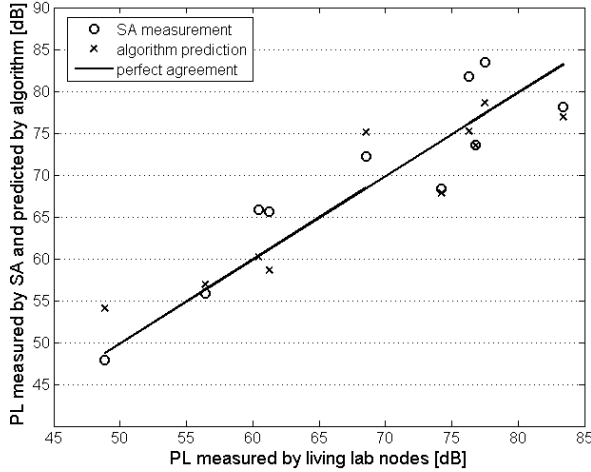

Fig. 5 Comparison of path loss measured by living lab nodes with path loss measured with spectrum analyser (SA) and with path loss predicted by propagation model for nodes grouped as in Fig. 4.

	Separate nodes		Grouped nodes	
	δ_{mean} [dB]	σ [dB]	δ_{mean} [dB]	σ [dB]
$PL_{pred}^{2.5\ m}$ - PL_{SA}	-1.87	6.96	-1.56	4.37
PL_{lab} - PL_{SA}	-2.14	6.81	-0.99	4.65
PL_{lab} - $PL_{pred}^{2.5\ m}$	-0.27	4.72	0.57	4.34

Table 5 Mean deviations δ_{mean} and standard deviations σ of the different predictions and measurements for the wireless living lab network.

8 Conclusions

A simple heuristic indoor path loss prediction algorithm for the 2.4 GHz-band has been developed. It bases its calculations on the dominant path between transmitter and receiver, but increases simplicity, introduces a strictly physical approach, and avoids neural networks and the accompanying need for a lot of training patterns. The algorithm, concept, and physical rationale have been presented. Measurements have been executed to construct and validate the model, on different floors of four buildings of different types. In contrary to many existing models no tuning of the model parameters is performed for the validation. Still, excellent correspondence between measurements and predictions is obtained: average absolute deviations for the different buildings vary between 1.29 dB and 3.08 dB, with standard deviations below 3.5 dB. The algorithm allows to quickly set up a new WLAN network for different types of indoor environments. The algorithm has also been applied to a WLAN living lab network with (fixed) nodes at specific locations. The average deviations remain low, but due to small-scale fading mechanisms, standard deviations increase up to around (maximally) 7 dB.

Future research could include an extension of the prediction algorithm for propagation through floors or ceilings and the development of an algorithm for automatic network optimization.

References

1. N. R. Prasad and M. Alam, "Security Framework for Wireless Sensor Networks," *Wireless Personal Communications*, vol. 37, no. 3-4, pp. 455–469, 2006.
2. S. Hamzah, M. Baharudin, N. Shah, Z. Abidin, and A. Ubin, "Indoor channel prediction and measurement for wireless local area network (WLAN) system," in *Communication Technology, 2006. ICCT '06. International Conference on*, Guilin, China, November 2006, pp. 1–4.

3. Zhong Ji and Bin-Hong Li and Hao-Xing Wang and Hsing-Yi Chen and T.K. Sarkar, "Efficient ray-tracing methods for propagation prediction for indoor wireless communications," *IEEE Antennas and Propagation Magazine*, vol. 43, no. 2, April.

4. Zhong Ji and Bin-Hong Li and Hao-Xing Wang and Hsing-Yi Chen and Yaw-Gen Zhau, "A new indoor ray-tracing propagation prediction model," in *Computational Electromagnetics and Its Applications, 1999. Proceedings. (ICCEA '99) 1999 International Conference on*, 1999, pp. 540–542.

5. Yinghua Li and Zhengwei Du and Ke Gong, "Comparison of different calculating methods for path loss in ray-tracing method at 2GHz," in *Microwave and Millimeter Wave Technology, 2004. ICMMT 4th International Conference on, Proceedings*, 18 - 21 August 2004, pp. 182–184.

6. M. D. R.P. Torres, L. Valle and M. Diez, "CINDOOR: an engineering tool for planning and design of wireless systems in enclosed spaces," *IEEE Antennas and Propagation Magazine*, vol. 41, no. 4, pp. 11–22, 1999.

7. G.M. Whitman and Kyu-Sung Kim and E. Niver, "A theoretical model for radio signal attenuation inside buildings," *IEEE Transactions on Vehicular Technology*, vol. 44, August 1995.

8. G. de la Roche, P. Flipo, Z. Lai, G. Villemaud, J. Zhang and J.-M. Gorce, "Combination of Geometric and Finite Difference Models for Radio Wave Propagation in Outdoor to Indoor Scenarios," in *3rd European Conference on Antennas and Propagation*, Barcelona, Spain, 12-16 April 2010.

9. L. Nagy, "Comparison and Application of FDTD and Ray Optical Method for Indoor Wave Propagation Modeling," in *3rd European Conference on Antennas and Propagation*, Barcelona, Spain, 12-16 April 2010.

10. J. Moreno Delgado, M. Domingo Gracia, J. Basterrechea Verdeja, J.R. Perez Lopez and L. Valle Lopez, "Automatic Channel and Aps Allocation in WiFi Networks Using Ray Tracing Techniques and Particle Swarm Optimization," in *3rd European Conference on Antennas and Propagation*, Barcelona, Spain, 12-16 April 2010.

11. G. Wlfle, R. Wahl, P. Wertz, P. Wildbolz, and F. Landstorfer, "Dominant path prediction model for indoor scenarios," in *German Microwave Conference (GeMIC)*, Ulm, Germany, April 2005.

12. A.G. Dimitriou and S. Siachalou and A. Bletsas and J.N. Sahalos, "An Efficient Propagation Model for Automatic Planning of Indoor Wireless Networks," in *3rd European Conference on Antennas and Propagation*, Barcelona, Spain, 12-16 April 2010.

13. M.B. Khrouf and M. Ayadi and S. Ben Romdhane and N. Saghrouni and S. Tabbane and Z. Belhadj, "Indoor Prediction of Propagation Using Dominant Path: Study and Calibration," in *Electronics, Circuits and Systems, 2005. ICECS 2005. 12th IEEE International Conference on*, Gammarth, December 2005.

14. P. Sebastiao, R. Tome, F. Velez, A. Grilo, F. Cercas, D. Robalo, A. Rodrigues, F. F. Varela and C. X. P. Nunes, "WLAN Planning Tool: a Techno-Economic Perspective," in *COST 2100 TD(09)935 meeting*, Vienna, Austria, 28-30 September 2009.

15. D. Plets, W. Joseph, L. Verloock, E. Tanghe, and L. Martens, "Evaluation of Indoor Penetration Loss and Floor Loss for a DVB-H Signal at 514 MHz," in *2010 IEEE International Symposium on Broadband Multimedia Systems and Broadcasting*, Shangai, March 2010, paper No. mm2010-04.

16. S. Todd and M. El-Tanany and G. Kalivas and S. Mahmoud, "Indoor radio path loss comparison between the 1.7 GHz and 37 GHz bands," in *Universal Personal Communications, 1993. Personal Communications: Gateway to the 21st Century. Conference Record., 2nd International Conference on*, vol. 2, Ottawa, Ont., October 1993, pp. 621–625.

17. S. Phaiboon, "An empirically based path loss model for indoor wireless channels in laboratory building," in *TENCON '02. Proceedings. 2002 IEEE Region 10 Conference on Computers, Communications, Control and Power Engineering*, vol. 2, October 2002, pp. 1020–1023.

18. T. Chrysikos and G. Georgopoulos and S. Kotsopoulos, "Site-specific validation of ITU indoor path loss model at 2.4 GHz," in *World of Wireless, Mobile and Multimedia Networks and Workshops, 2009. WoWMoM 2009. IEEE International Symposium on a*, Kos, 15-19 June 2009, pp. 1–6.

19. A. Durantini and D. Cassioli, "A multi-wall path loss model for indoor UWB propagation," *Vehicular Technology Conference, 2005. VTC 2005-Spring. 2005 IEEE 61st*, vol. 1, pp. 30–34, 30 May - 1 June 2005.

20. R.S. de Souza and R.D. Lins, "A new propagation model for 2.4 GHz wireless LAN," in *Communications, 2008. APCC 2008. 14th Asia-Pacific Conference on*, Tokyo, Japan, 14-16 October 2008, pp. 1–5.

21. G.J.M. Janssen and R. Prasad, "Propagation measurements in an indoor radio environment at 2.4 GHz, 4.75 GHz and 11.5 GHz," *Vehicular Technology Conference, 1992, IEEE 42nd*, vol. 2, pp. 617–620, 10 May - 13 May 1992.

22. C. Perez-Vega and J.L. Garcia, "A Simple Approach to a Statistical Path Loss Model for Indoor Communications," in *Microwave Conference, 1997. 27th European*, vol. 1, Jerusalem, Israel, 8 - 12 September 1997, pp. 617–623.

23. Jae-Woo Lim and Yong-Sub Shin and Jong-Gwan Yook, "Experimental performance analysis of IEEE802.11a/b operating at 2.4 and 5.3 GHz," in *Communications, 2004 and the 5th International Symposium on Multi-Dimensional Mobile Communications Proceedings. The 2004 Joint Conference of the 10th Asia-Pacific Conference on*, vol. 1, 29 August - 1 September 2004, pp. 133–136.

24. S. Phaiboon and P. Phokharatkul and S. Somkuarnpanit and S. Boonpiyathud, "Upper- and lower-bound path-loss modeling for indoor line-of-sight environments," in *Microwave Conference Proceedings, 2005. APMC 2005. Asia-Pacific Conference Proceedings*, vol. 4, 4-7 December 2005.

25. J. Jemai and R. Piesiewicz and T. Kurner, "Calibration of an indoor radio propagation prediction model at 2.4 GHz by measurements of the IEEE 802.11b preamble," in *Vehicular Technology Conference, 2005. VTC 2005-Spring. 2005 IEEE 61st*, vol. 1, 30 May - 1 June 2005, pp. 111–115.

26. R. Tahri and V. Guillet and J.Y. Thiriet and P. Pajusco, "Measurements and Calibration Method for WLAN Indoor Path Loss Modelling," in *3G and Beyond, 2005 6th IEE International Conference on*, 7-9 November 2005, pp. 1–4.

27. W. Joseph, L. Verloock, D. Plets, E. Tanghe, and L. Martens, "Characterization of coverage and indoor penetration loss of DVB-H signal of indoor gap filler in UHF band," *IEEE Transactions on Broadcasting*, vol. 55, no. 3, pp. 589–597, 2009.

28. F. Capulli and C. Monti and M. Vari and F. Mazzenga, "Path Loss Models for IEEE 802.11a Wireless Local Area Networks," in *Wireless Communication Systems, 2006. ISWCS '06. 3rd International Symposium on*, Valencia, Spain, 6-8 September 2006, pp. 621–624.

29. J.-F. Wagen, "Indoor Service Coverage Predictions: How Good is Good enough?" in *3rd European Conference on Antennas and Propagation*, Barcelona, Spain, 12-16 April 2010.

30. L. Stola, G. Urso, and P. Tenani, "Indoor propagation: Experimental validation at 1.7 GHz of a UTD-based approach," *Wireless Personal Communications*, vol. 3, no. 3, pp. 225–241, 1996.

31. D. Plets, W. Joseph, K. Vanhecke, E. Tanghe, and L. Martens, "Development of an Accurate Tool for Path Loss and Coverage Prediction in Indoor Environments," in *European Conference on Antennas and Propagation 2010*, Barcelona, 12-16 April 2010.

32. G. Wlfle, F. Landstorfer, R. Gahleitner, and E. Bonek, "Extensions to the field strength prediction technique based on dominant paths between transmitter and receiver in indoor wireless communications," 1997.

33. G. Berger, R. Goedeken, and J. Richardson, "Motivation and Implementation of a Software H.264 Real-Time CIF Encoder for Mobile TV Broadcast Applications," *IEEE Transactions on Broadcasting*, vol. 53, no. 2.

34. Mat Equipement, "MA431Z00, 2400..2485 MHz, 4 dBi," Tech. Rep. [Online]. Available: http://www.gigacomp.ch/pdfs/MatJaybeam_MA431Z00.pdf

35. Y. E. Mohammed, A. Abdallah, and Y. A. Liu, "Characterization of Indoor Penetration Loss At ISM Band," in *Asia-Pasific Conference on Environmental Electromagnetics CEEM'2003*, Hangzhou, China, Nov. 2003, pp. 25– 28.

36. Y. Zhang and Y. Hwang, "Measurements of the characteristics of indoor penetration loss," in *Vehicular Technology Conference, 1994 IEEE 44th*, vol. 3, Stockholm, Sweden, Jun. 1994, pp. 1741–1744.

37. G. Tesserault and N. Malhouroux and P. Pajusco, "Determination of Material Characteristics for Optimizing WLAN Radio," in *Wireless Technologies, 2007 European Conference on*, Munich, Germany, 8-10 October 2007, pp. 225–228.
38. A. Turkmani and A. de Toledo, "Modelling of radio transmissions into, and within buildings at 900, 1800 and 2300 MHz," *IEE Proceedings*, vol. 140, no. 6, pp. 462–470, Dec. 1993.
39. N. Papadakis, A. Economou, J. Fotinopoulou, and P. Constantinou, "Radio Propagation Measurements and Modeling of Indoor Channels at 1800 MHz," *Wireless Personal Communications*, vol. 9, no. 2, pp. 95–111, 1999.
40. A. Martinez, D. Zabala, I. Pena, P. Angueira, M. Velez, A. Arrinda, D. de la Vega, and J. Ordiales, "Analysis of the DVB-T Signal Variation for Indoor Portable Reception," *IEEE Transactions on Broadcasting*, vol. 55, no. 1, pp. 11–19, March 2009.
41. G. Steinbock, T. Pedersen and B. H. Fleury, "Model for the Path Loss of In-room Reverberant Channels," in *COST 2100 TD(10)11057 meeting*, Aalborg, Denmark, 2-4 June 2010.